

Eleventh Quarterly Progress Report

February 1, 2009 to April 30, 2009

Contract No. HHS-N-260-2006-00005-C

Neurophysiological Studies of Electrical Stimulation for the Vestibular Nerve

Submitted by:

James O. Phillips, Ph.D.^{1,3,4}

Steven Bierer, Ph.D.^{1,3,4}

Albert F. Fuchs, Ph.D.^{2,3,4}

Chris R.S. Kaneko, Ph.D.^{2,3}

Leo Ling, Ph.D.^{2,3}

Shawn Newlands, M.D., Ph.D.⁵

Kaibao Nie, Ph.D.^{1,4}

Jay T. Rubinstein, M.D., Ph.D.^{1,4,6}

¹ Department of Otolaryngology-HNS, University of Washington, Seattle, Washington

² Department of Physiology and Biophysics, University of Washington, Seattle, Washington

³ Washington National Primate Research Center, University of Washington, Seattle, Washington

⁴ Virginia Merrill Bloedel Hearing Research Center, University of Washington, Seattle, Washington

⁵ Department of Otolaryngology, University of Rochester, Rochester, New York

⁶ Department of Bioengineering, University of Washington, Seattle, Washington

Reporting Period: February 1, 2009 to April 30, 2009

Challenges:

1. We still have not received an adequate supply of axial multiple single unit recording electrodes. As of the end of Quarter 11, we still had not received multiple single unit axial recording electrodes from Neuronexus – FHC. We did have several discussions with both Neuronexus and FHC during Quarter 11 about the electrode design and the limitations that they have encountered in the fabrication of our electrodes. Fundamentally, they cannot deliver on the original design specifications. The most critical of these is the diameter of the shaft of the electrode that must fit in our recording cannula. The electrodes have a connection point midway down the shaft of the tungsten electrode core that must be insulated with heat shrink tubing, thus increasing its diameter beyond the inner diameter of our recording cannula.

In response to this technical issue, we agreed early in Quarter 11 to accept a first production run of larger diameter electrodes that otherwise approximated the original design specifications. We explored the use of an ultrathin cannula that would accommodate such an electrode design, but found these to be too weak and brittle for our application. We then revised the design of our cannula, microdrive, and cannula guides to accept larger electrodes. Basically, we now have the capability to use the larger electrodes in this modified recording apparatus. Unfortunately, Neuronexus - FHC delivered only two prototypes of the larger axial electrode design by the end of the first month of Quarter 12. We are optimistic that our investment in redesign will be rewarded by the arrival of the additional electrodes in Quarter 12. In the mean time, we will continue to use our locally fabricated tungsten microelectrodes and Thomas recording GMBH tetrodes for our continuing and successful recording experiments.

2. During a reimplantation of a monkey with a minimally invasive vestibular prosthesis of the original design, we eliminated vestibular and hearing function in the implanted ear. We suspect that the aggressive implantation of the device through an oversized fenestration close to the ampulla of the implanted canal produced a rupture of the membranous labyrinth and subsequent loss of hair cell function in that ear. Although the animal did not appear distressed immediately following the implantation, and indeed continues to work well with no overt signs of functional loss on direct observation, rotational testing revealed a loss of vestibular function in the implanted ear. Absence of an auditory evoked potential in this monkey (monkey S3 below) revealed a loss of hearing in that ear without obvious signs of a conductive hearing loss.

Our response to this challenge was and is to fully document the function of our prosthesis following loss of hair cell function in an implanted ear. Indeed, this is somewhat serendipitous because we have demonstrated that the device continues to drive overt behavioral responses in an otherwise nonfunctional ear (i.e., an ear without apparent intact hair cell function). The responses are virtually identical to the responses in monkeys with intact vestibular function and hearing. Vestibular electrically evoked

compound action potentials (vECAP) were also obtained in this animal at low stimulus thresholds during and after surgery. Overall, we feel that this data confirms our impression that our implant is driving vestibular afferents directly, and that hair cell activation is not required for the device to function effectively (see below).

Current Successes:

1. We have received our redesigned vestibular prosthesis from Cochlear Corporation. The new prosthesis has elongated leads and stimulation sites, which simplify the placement and fixation of the device and expand, by 50%, the area of each stimulation site. The device design was described in our Ninth Quarterly Progress Report. These devices have a lower theoretical impedance. This was confirmed with in vivo impedance measurement following implantation of a single a monkey with the new device.

2. We have performed two additional implantations of the vestibular prosthesis using NRT-guided minimally invasive technique. Both of these implantations were approved revision surgeries on animals with non-working prostheses. The revision surgery in one of these animals resulted in a vestibular implant that produced electrically elicited eye movements at low thresholds in an ear that had normal auditory brainstem responses (ABR) and normal vestibular function during testing. vECAP was obtained at low stimulus thresholds during and after surgery. The newer redesigned device was implanted in this animal. The animal has a neural recording chamber and we are currently recording single neuron activity after fully characterizing the animal's behavioral response to electrical stimulation.

A second animal was implanted with an older design device during a revision surgery. vECAP was obtained at low threshold during the surgery in both implanted canals (lateral and posterior). Immediately following surgery, vECAP was weakly present at high threshold in one implanted canal, and absent in the other. The animal retained natural vestibular function and ABR post surgically. The implanted device did not produce electrically elicited eye movements from stimulation in either implanted canal. Recording of electrical artifact using surface electrodes suggests that the device itself is functioning properly, but that the leads have shifted or were pulled out of the fenestrations in the bony labyrinth during or immediately following implantation.

3. We performed extensive testing on a third animal implanted before the start of Quarter 11. This animal, as mentioned above, had a revision surgery that eliminated hearing and natural vestibular function in the implanted ear. The implanted device produces electrically elicited eye movements at low thresholds in the implanted ear, but the surgery dramatically reduced the ABR and measured vestibular function in that ear. The older design device was implanted in this animal. We are currently recording single neuron activity after fully characterizing the animal's behavioral response to electrical stimulation, which was similar to that of other animals with intact ABR and vestibular function.

In this animal we have found that we can elicit vECAP at low thresholds. Changes in frequency and amplitude of trains of electrical stimuli change the slow phase velocity of the electrically elicited nystagmus. The current thresholds required for nystagmus are low, on the order of 50 μ A, and similar to the thresholds required for stimulation of the intact ear in other monkeys. Also, we have been able to drive neurons in the brainstem of this monkey. Tonically active neurons, that do not respond to head rotation because of the loss of hair cell function in the ear ipsilateral to the recording, have been driven at monosynaptic latency at the location, in the brainstem, of the maximal electrically evoked field potential elicited by the prosthesis. This location overlaps the location of vestibular nuclei relative to the functionally identified abducens nucleus ipsilateral to the implanted canal, and will be confirmed histologically by reconstruction of electrolytic lesions at the end of the experiments. The threshold for activation of these neurons was at the threshold for activation of the overt behavior (50 μ A). As stated above, we feel this is evidence that the vestibular prosthesis drives the vestibular afferents directly at the end organ.

4. We have performed auditory brainstem response (ABR) recording in all 6 implanted monkeys. A potential complication of implant surgery is hearing loss. Mechanical and thermal insults, as well as vibrations from drilling, can damage the vulnerable auditory structures of the inner ear, a risk exacerbated by the close proximity and shared fluid space of the semicircular canals and the cochlea.

The auditory brainstem response (ABR) is a widely used clinical tool to diagnose hearing problems in humans, and has been extensively employed in research to assess auditory function in animals, including the rhesus macaque. We recorded ABRs this quarter in all six implanted monkeys. The animals were first sedated with a mixture of ketamine (7-14 mg/kg) and xylazine (0.6-1.2 mg/kg). An otoscopic examination was performed to assess the status of the middle ear, and accumulated debris was removed from the ear canal if necessary. Acoustic condensation clicks (100 ms phase, repeated 300-500 times at a rate of 10/sec) were generated with a PC sound card controlled by custom software and delivered via infant-size earphones inserted into the ear canal. The unattenuated click intensity was approximately 120 dB pSPL (referred to a pure tone having the same peak calibration voltage), based on calibration with a 1/4" probe microphone (Larson-Davis) in a 0.5 cc sealed volume. Evoked potentials were recorded from the scalp with subdermal electrodes placed at the vertex (+), ipsilateral mastoid (-), and contralateral mastoid (ground). The recorded signal was amplified using a gain of 10,000 at a bandwidth of 100-3000 Hz, digitized by the sound card, and averaged for analysis in the custom software. ABRs were obtained successively from both ears, with an earplug placed in the non-test ear.

An example ABR waveform from one animal (S1) is displayed in Fig. 1. This animal had a functioning vestibular implant in the right ear, with electrode arrays implanted in the lateral and posterior semicircular canals. No implantation or other temporal bone surgery was conducted on the left side. The ABR in Fig. 1 was made in response to a high intensity click (0 dB attenuation) presented to the left ear. After the artifact at time 0 ms, several distinct positive and negative peaks occur with latencies between ~1.8 and 5 ms, followed immediately by a broad wave sloping from negative to positive. The

waveform closely resembles ABRs recorded in the rhesus macaque by other investigators. We have used a labeling convention of the positive peaks (waves I-IV) in Fig. 1 that follows earlier papers.

ABRs obtained at various levels of attenuation in the same animal are shown in Fig. 2A (left ear) and Fig. 2B (right ear). As click level decreased, the ABR peaks decreased in amplitude and increased in latency. Note that the overall ABR amplitudes are smaller for the right ear. Determination of threshold was based on Wave IV, as this tended to be the largest peak at low intensities for all the animals tested. Threshold was subjectively defined as the minimum current eliciting a clear positive-to-negative excursion, near the expected Wave IV latency, that is clearly larger than the background noise. In this example, the threshold was -80 dB for the left (unimplanted) ear and -65 dB for the right (implanted) ear. A 15 dB difference in threshold suggests a moderate conductive hearing loss in the right ear (see Table 1), but otherwise indicates proper signal transduction in the inner ear and along the cochlear branch of the eighth nerve to the brainstem. This example demonstrates that hearing can be preserved following a successful implantation of one or more semicircular canals.

Table 1 summarizes the ABR results of all the animals. The thresholds of the unimplanted contralateral ears ranged from -80 to -60 dB (40 - 60 dB pSPL) for all animals except S5 (see below). This range is comparable to ABR thresholds of normal adult rhesus monkey obtained in other studies. Three of the six monkeys had implanted ipsilateral ear thresholds lower than -60 dB. Two of the remaining three (S2 and S6) showed indication of a mild conductive hearing loss during otoscopic examination, and thresholds 20-25 dB higher in the implanted ear. In the final animal (S3), the difference in threshold was greater than 70 dB, strongly suggesting sensorineural hearing loss in the implanted ear. This animal had a working implant, but no vestibular function in the implanted ear.

An ABR could not be measured from the left ear of animal S5. Prior to ABR measurement in this animal, we had performed 8th nerve single unit recording on the left side with tungsten microelectrodes. We believe that the 8th nerve was damaged during one of these recording sessions, because the microelectrode was bent and hooked when it was removed after a recording session. ABRs were successfully obtained in the implanted ear, and the low ABR threshold suggests that the vestibular implant surgery did not adversely affect auditory function. This example also demonstrates that any acoustic energy conveyed by bone conduction to the non-test ear does not contribute appreciably to the recorded ABRs.

Overall, in two of four animals that received implantation with the minimally invasive technique and UW-Cochlear vestibular prosthesis, there were no significant differences in hearing function between the implanted and unimplanted ear. In one animal there was an indication of a mild conductive hearing loss following such a surgery, and one animal lost hearing after reimplantation. In the two animals who received canal plugging and fine wire electrodes, one animal had a mild conductive hearing loss in the implanted ear, and one had normal hearing in the implanted ear.

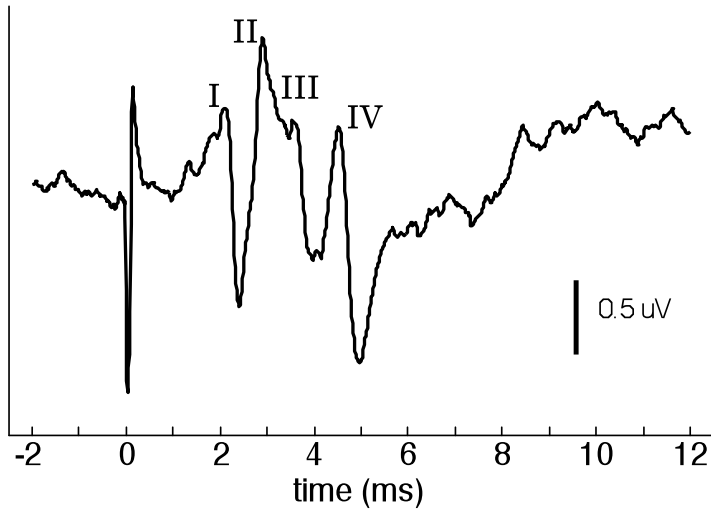


Figure 1. ABR recording obtained from high intensity click stimulation of a non-implanted ear in a rhesus monkey.

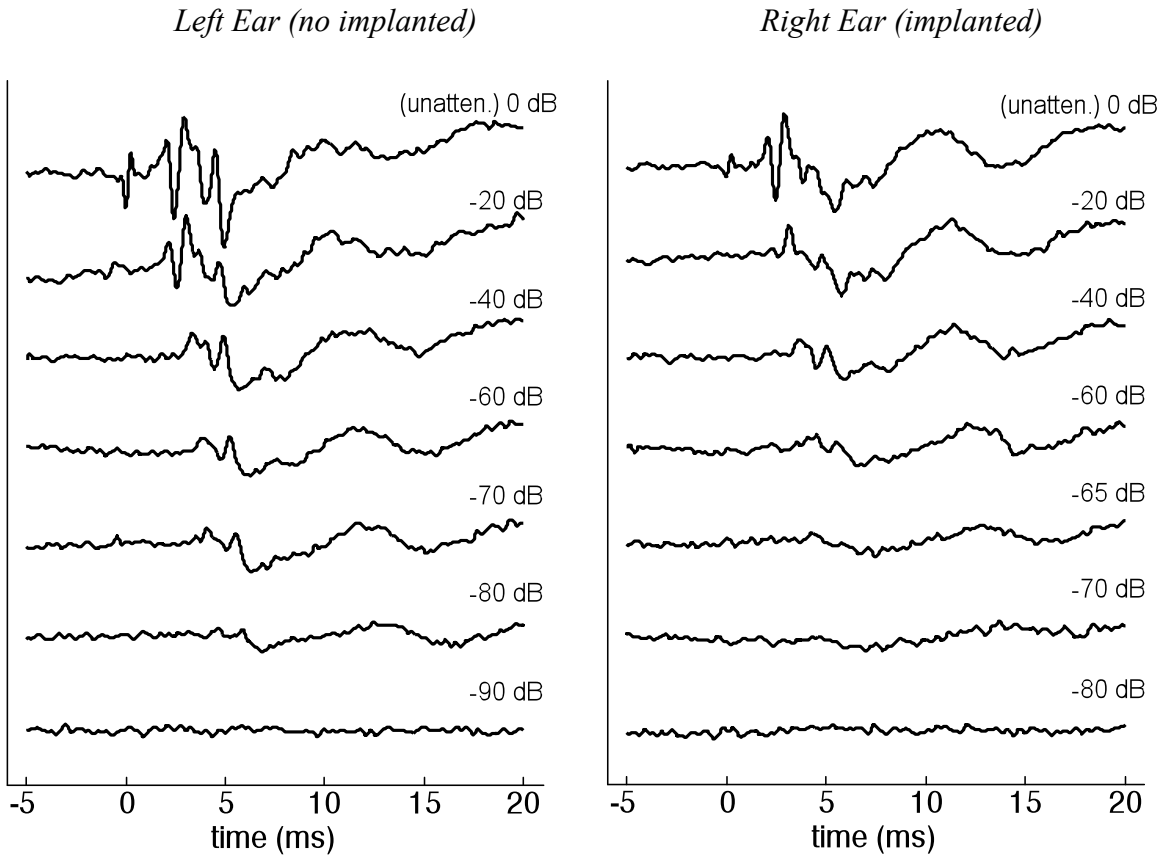


Figure 2. Comparison of the responses elicited at different click intensities by stimulation of the non-implanted and implanted ears of the monkey in Fig. 1.

Animal ID	Type of Surgery	# Functioning Channels	Contra Thr.	Ipsi Thr.	Ear Condition
S1	MI/REV	2	-80	-65	Ipsi: tympanic membrane not visible
S2	MI/REV	2	-60	-35	Ipsi: tympanic membrane not visible
S3	MI/REV	1	-75	-5*	Ipsi, Contra: OK
S4	MI/REV	0	-75	-70	Ipsi, Contra: OK
S5	CP	1	None*	-70	Contra: 8 th n. destroyed
S6	CP	2	-60	-40	Ipsi: inflammation in external canal

*Table 1. Summary of ABR measurements. **MI/REV** indicates that the animal had received a minimally invasive revision surgery with the UW Cochlear device before testing. **CP** indicates that the animal had received canal plugging and fine wire insertion before testing. * indicates probable SNHL. **Contra** indicates the ear contralateral to implantation. **Ipsi** indicates the ear ipsilateral to implantation. **Ear Condition** reports the result of otoscopic evaluation of the ears.*

5. We have obtained behavioral results during neural response telemetry (NRT) stimulation in our animals. Previously, we had obtained vECAP in our animals and had correlated the result of this recording with the presence of electrically evoked eye movements using different stimulus trains in separate experiments in the same animal. Fig. 3 shows the result of eye movement recording during NRT stimulation that produces vECAP. This figure shows that NRT stimulation, with a masking stimulus, produces transient increases in eye velocity associated with the current pulses, and a nystagmus. In Fig. 3A, the current is adjusted to the level which is just above threshold for production of a vECAP. In figure 3B, the current is suprathreshold, producing higher transient velocity peaks and a higher slow phase velocity. This demonstrates that the vECAP NRT stimulus produces both a vECAP and a behavioral response that scales with the evoked compound action potential.

6. We have obtained and are testing a modified PDA based stimulation technology for our prosthesis from Dr. Philip Loizou at University of Texas, Dallas. The device, shown in Fig. 4, consists of a revised PDA SDIO interface board, with an upgrade in its FPGA, which can potentially solve some of the problems we encountered in our previous animal experiments. We first tried this board on the Dell PDA that we previously used, and we found some software compatibility issues. We ordered a new PDA (HP iPAQ hx2790), and testing and programming is in progress.

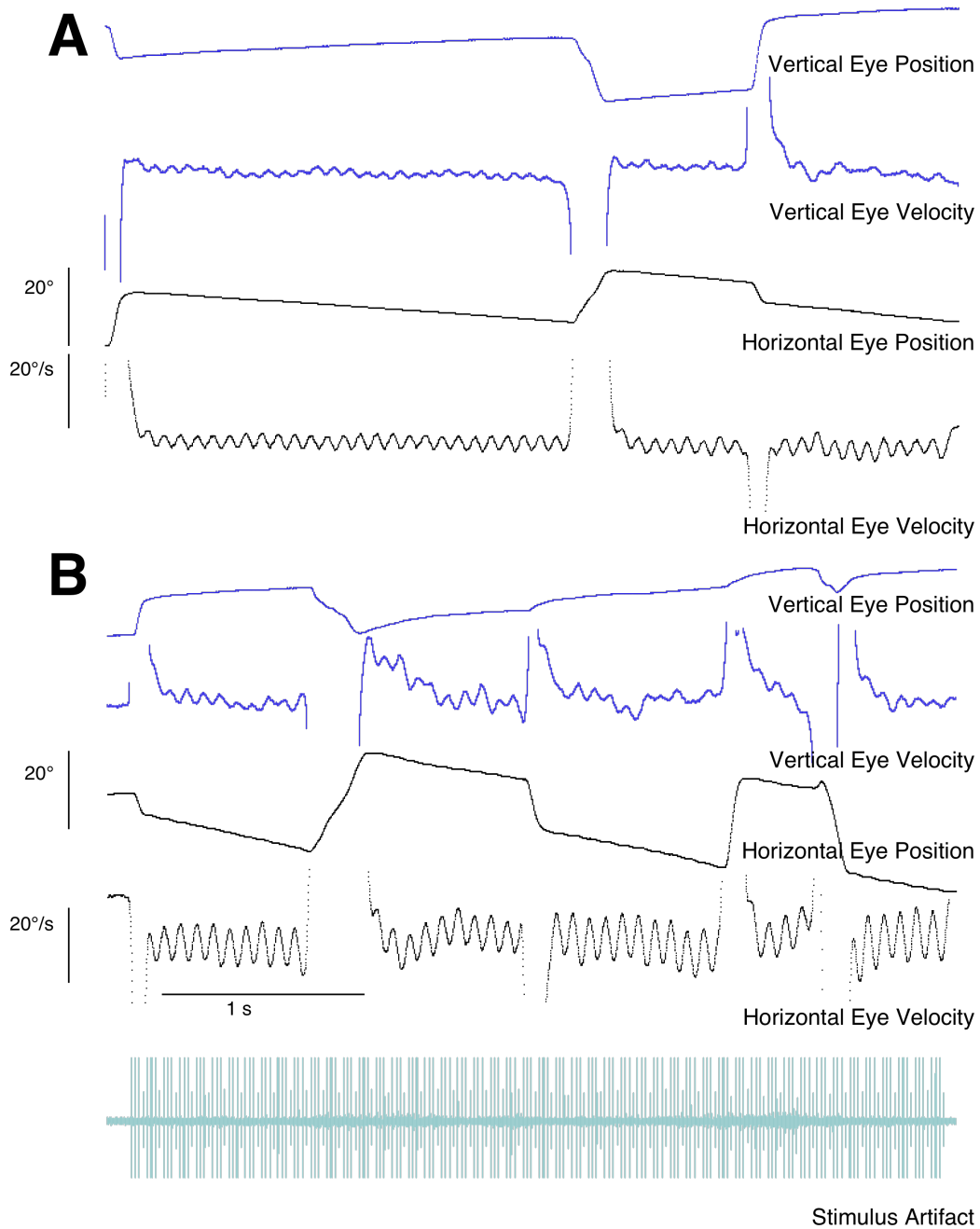


Figure 3. Eye movements resulting from NRT of a lateral canal electrode in a rhesus monkey in response to a low current stimulation (70 CU) in A, and higher current stimulation (100CU) in B.

7. In this quarter, we tested the feasibility of driving our vestibular implants in real time with a standard clinical cochlear implant processor. The clinical processor has the capability of taking audio inputs and converting them into amplitude modulated (AM) pulse trains in real time. Normally, the rotational signals that eventually would drive a vestibular implant have frequencies below 10 Hz, which are equivalent to AM signals in nature. We can modulate the low-frequency rotational signals with a 1000-Hz carrier to generate an analog signal that can be fed into the direct audio input of a cochlear implant sound processor. The AM signals can then pass through a series of signal processing blocks in cochlear implants and pulse trains with the same AM signals can be reconstructed on a target electrode.

A signal-channel map was created using the standard clinical fitting software—Custom Sound V2.0. Fig. 5 shows the graphical user interface used to create the map. In the map, only electrode 9 was enabled to process the 1000-Hz amplitude modulated input analog signals. The minimum current level (threshold) was set to 0 and the maximum current level was set to 110 clinical levels to be consistent with our findings in previous stimulation experiments using the NIC2 pulse train generator. The pulse rate was at 250 pulses/sec and the pulse width was 100 μ s per phase. The frequency range was from 188 to 1063 Hz, which was sufficient to cover the frequency spectrum of the 1-kHz modulated input signal.

In addition, any signal processing functions in cochlear implants that can potentially alter the AM signals or generate noise in pulse trains, was either set to ‘off’ or was minimized by carefully choosing the parameter settings. The ratio of auxiliary to microphone input was set to 10:1 and the microphone sensitivity was fixed at the lowest level, —0—, to suppress any background noise when the microphone is still active. The Nucleus processors do not allow the microphone inputs to be switched off. The ADRO (Adaptive Dynamic Range Optimization) was also set to ‘off’ to avoid any distortions created by this automatic gain control process. Most importantly, we changed the compression function to a nearly linear curve by setting the value of Q to 50 (maximum allowed). This modification allows μ s to minimize the effect of nonlinear compression on the envelope of pulse trains and thus we can obtain the modulated pulse trains at a similar modulation depth. The default Q value is 20 in standard cochlear implant fittings. Figure 6 shows the effects of changing Q value on the input-output relationship. As Q increases from 20 to 50, the relationship between filter envelope amplitude and output magnitude is somewhat linearized, as can be seen in the Q=50 curve.

In our experiments, a Nucleus Freedom speech processor was used to drive the implanted device on one of our monkeys. The 1000-Hz modulated signal was connected to the auxiliary input jack of the processor through a dedicated audio cable. Prior to conducting stimulation experiments, the processor was programmed with the single-channel map described above and the output current was calibrated with respect to the peak voltage of the AM analog input signal. For the example in Fig. 7, we adjusted the parameters of the input analog AM signal to achieve a peak current of 45 μ A in the output AM pulse train. The input modulation depth was 60%, which resulted in a ~50% modulation depth for the output pulse train.

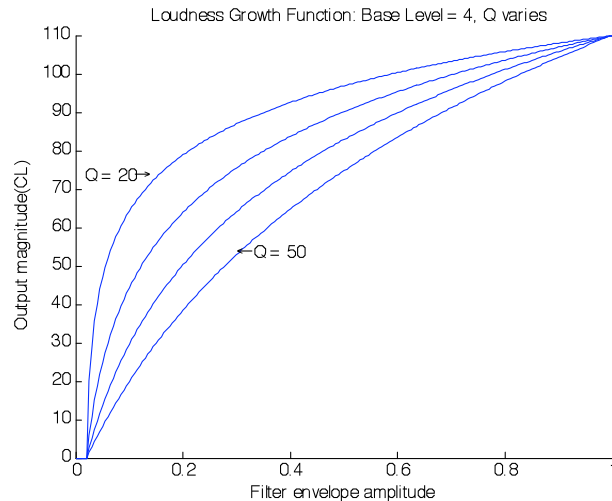
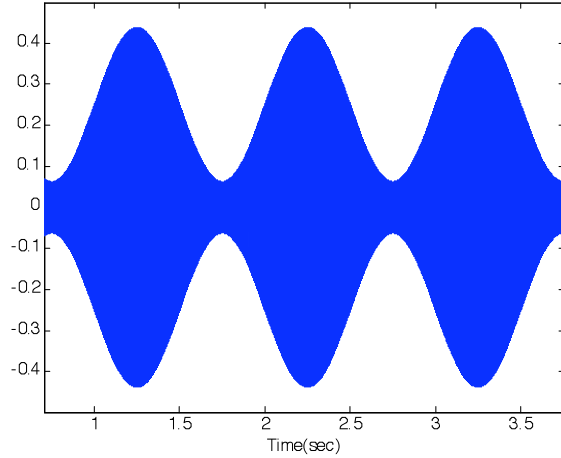


Figure 6: Output magnitude in CL (Clinical Level) versus normalized filter envelope amplitude as a function of changing Q from 20 to 50.

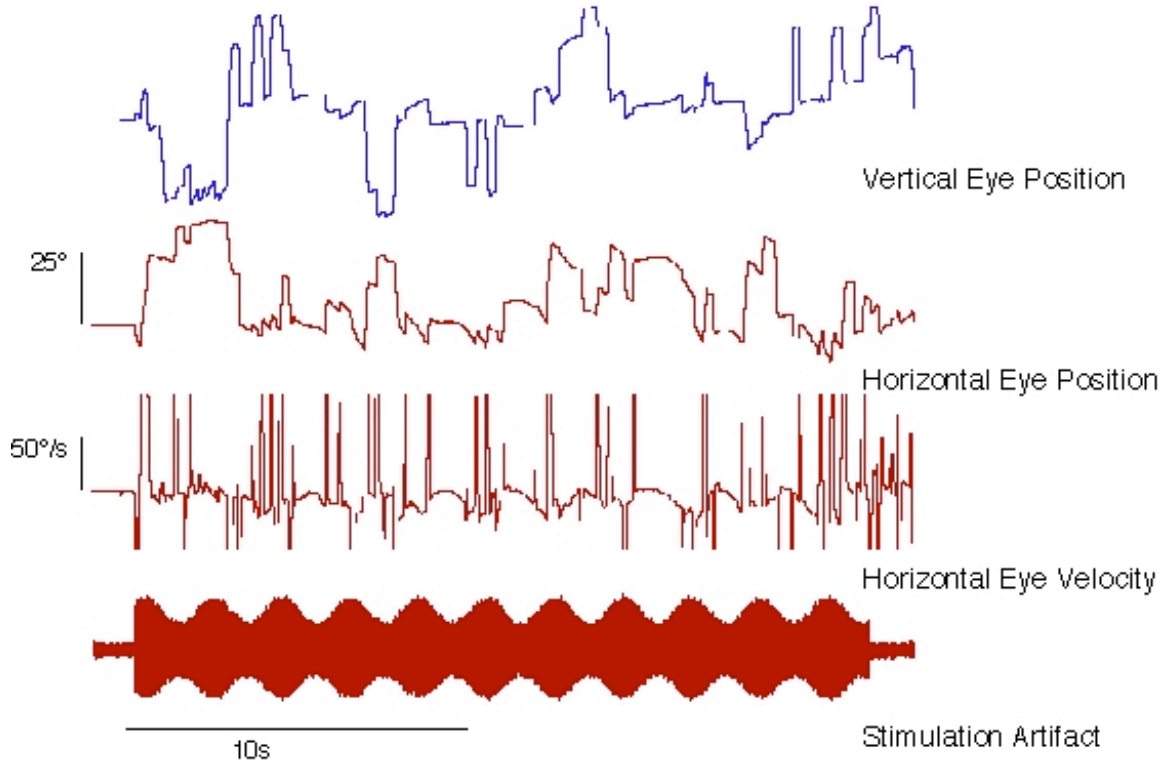
In Fig. 7, a 0.5 Hz sinusoidally modulated analog input produced sinusoidally modulated eye velocity output predominantly in the plane of the stimulated canal. This eye movement was generated in real time from an analog input, demonstrating the feasibility of using this approach to have head velocity signals from the coil system drive compensatory eye movement.

8. In this quarter, we used the vestibular prosthesis to null ongoing vestibular nystagmus. One potential application of this vestibular prosthesis is to compensate for acute loss of vestibular input from an ear during an attack of vertigo in Meniere's disease. For this to be an effective strategy, the device must be capable of cancelling an ongoing imbalance in vestibular input. While an animal model of reversible vestibular imbalance due to transient loss of vestibular function was not practical in our monkeys, we did produce an experimental analog of the whirling vertigo experienced by patients during an attack. In a series of experiments we rotated the animal en-bloc with a slowly accelerating vertical axis rotation stimulus. This produced a robust nystagmus with a sustained peak velocity. We then applied a constant frequency stimulus to the lateral canal to generate nystagmus of equal velocity in the opposite direction. The stimulation parameters were calculated from the frequency and current versus slow phase velocity series conducted earlier for the stimulated electrode. The result is shown in Fig. 8, which displays the eye position and velocity resulting from the nulling of a rotation induced nystagmus. During the stimulation train (black bar), the slow phase eye velocity drops to 0 deg/s for the duration of the stimulation.

9. In this quarter, we continued our stimulation and recording experiments and demonstrated several important characteristics of the processing of electrical stimulation by neurons in the vestibular nucleus. First, we expanded our sample of recorded neurons by recording in 2 additional animals. Second, at high currents, we were able to drive a few neurons that had vertical rotation sensitivity with electrical stimulation



A.



B.

Figure 7. Real time amplitude modulated electrically elicited eye movements from stimulation of the lateral canal. Inset A displays the 0.5 Hz amplitude modulated analog input signal superimposed on a 1000 Hz carrier. B shows the eye position and velocity, and the amplitude modulated stimulation artifact, resulting from the stimulation.

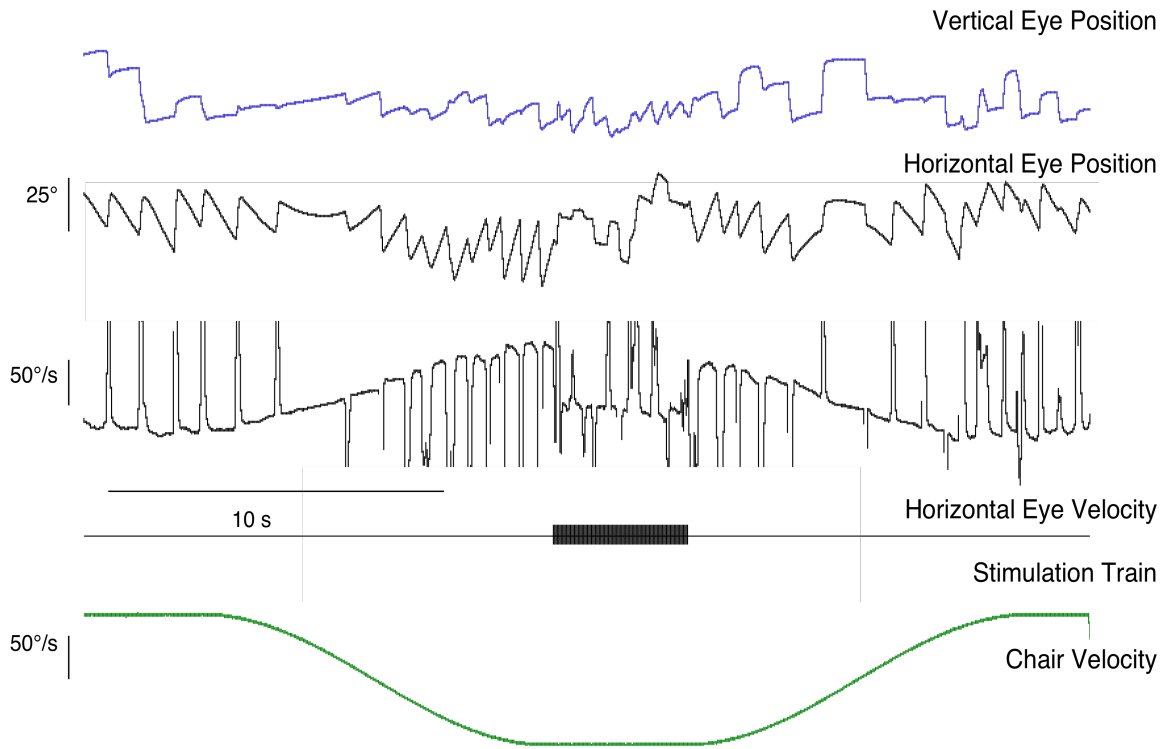


Figure 8: Nulling of ongoing vestibular induced nystagmus with a stimulation train applied to a lateral canal electrode.

of a lateral canal electrode. These neurons all had canal sensitivity consistent with natural stimulation of the superior canal. Third, we continued to observe that individual driven neurons have a relatively consistent threshold, which is approximately the threshold stimulus for electrically elicited slow phase eye movements (e.g., 50 μ A). The absence of a significant range of thresholds was unexpected, because it suggests that simple recruitment of individual vestibular neurons cannot underlie the amplitude modulation of slow phase eye velocity during electrical stimulation. Fourth, we observed that the threshold does not change with stimulation current across a broad range of stimulation frequencies. We determined the threshold for individual neurons during a 10 Hz stimulus train, and then checked the threshold at 50, 100 and 200 Hz. Individual neurons showed similar thresholds throughout this frequency range.

Fifth, we examined the frequency following of individual vestibular neurons at just above threshold and well above threshold. We observed that single neurons followed electrical stimulation to frequencies of up to 400 Hz, which was the highest frequency that our recording amplifier could follow units driven at monosynaptic latency. Using software developed in previous quarters, we were able to sort the somatic spikes of single neurons from the stimulus artifact, and study the consistency of the response to electrical stimulus trains at high frequencies. Fig. 9 displays one such experiment. In figure 9, a single

neuron is recorded along with the artifact of the electrical stimulation that is driving that neuron. The analysis software isolates the recorded unit activity in red (either the neuron or the stimulus artifact), and rejects the unit activity in grey. The instantaneous rate of the selected unit activity is displayed above the corresponding recording traces. Figure 9 shows that at 2X threshold stimulus current the frequency of firing of the vestibular neuron follows the frequency of the stimulus.

In Fig. 10, the firing of the same neuron is displayed at higher temporal resolution during the high frequency portion of the modulated stimulus train. The neuron discharge reliably follows the stimulus artifact at a consistent latency and is partially superimposed on the vestibular field potential. A smaller vestibular neuron spike is occasionally seen at a longer and somewhat variable latency following the stimulus artifact. It is unclear whether this response is a doublet or represents the recruitment of a second neuron at longer latency.

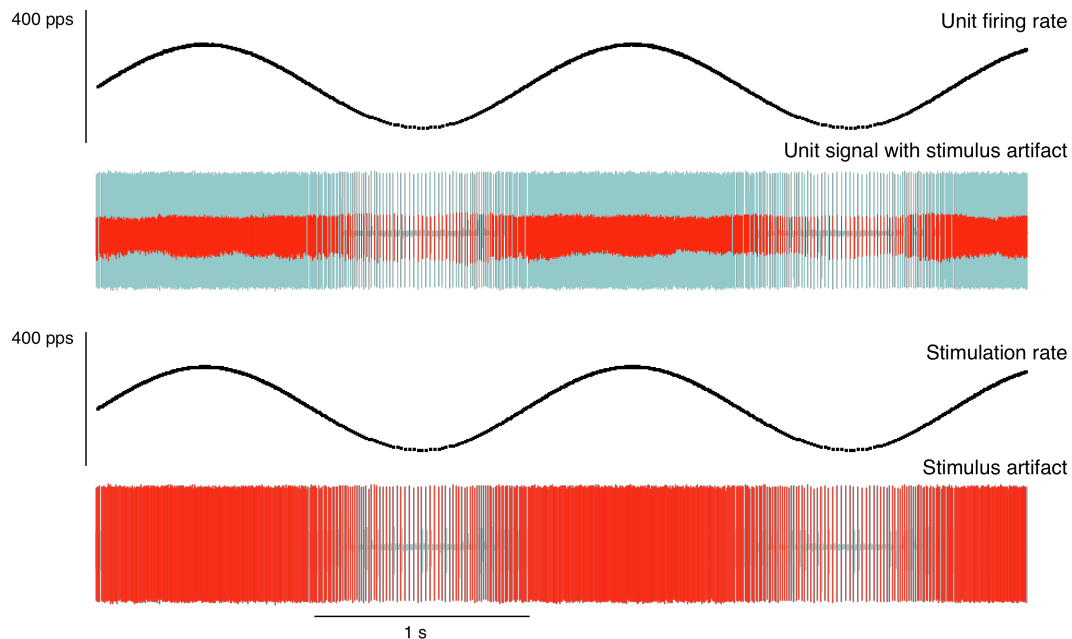


Figure 9: Unit firing rate relative to stimulation rate for a single neuron recorded during 0.5 Hz sinusoidal frequency modulation of a 100 μ A (2X threshold) stimulation train. Stimulus frequency varied from 50 to 300 pps. Stimulation parameters were 100 μ s pulse width, 8 μ s gap, stimulating the distal electrode in the right lateral canal. Stimulation and unit instantaneous firing rates were obtained by identifying the stimulus artifact or single neuron (single unit) displayed in red, and rejecting the other recorded spikes (in grey).

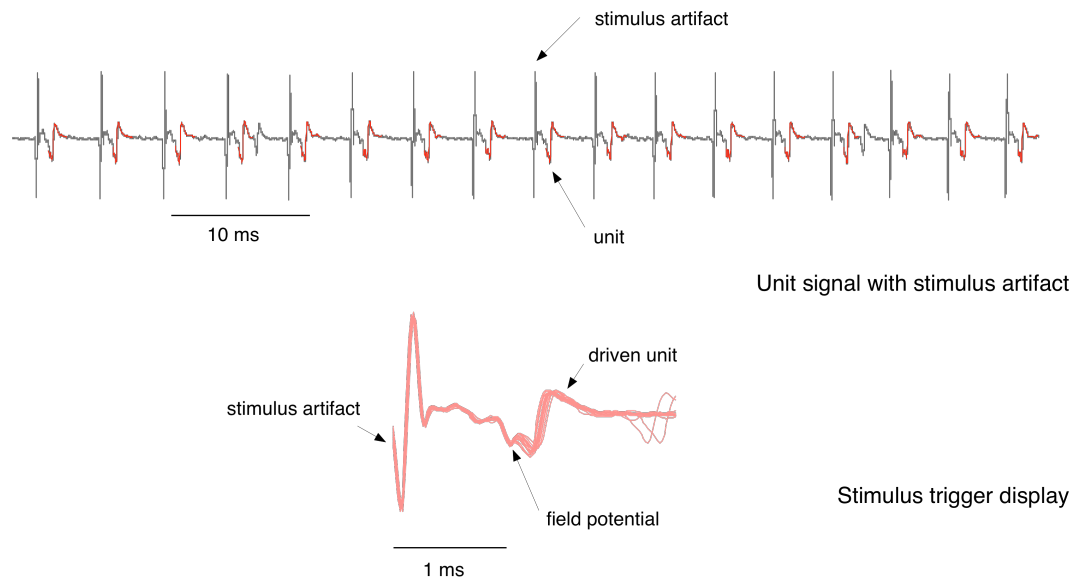


Figure 10: Stimulation of the single vestibular neuron shown in Fig. 9 with a high frequency stimulation train at 2X threshold current. The vestibular neuron (red) follows each stimulus pulse (grey) with a single spike discharge. Occasionally a second spike is seen at a longer latency in response to the stimulus, but the latency is inconsistent and spike amplitude is different from that of the target neuron as seen in the stimulus triggered display in the inset below.

At threshold stimulus of 50 μA , the frequency following of the same vestibular neuron breaks down at higher frequencies, despite the fact that this neuron showed a consistent threshold at frequencies from 10 to 200 Hz. In response to a 0.5 Hz sinusoidal stimulus, modulated from 50 to 300 pps, the instantaneous firing rate shows the occasional drop out of individual spikes as a $\frac{1}{2}$ decrement in neuron discharge frequency at high stimulus frequency (Fig. 11A). The stimulus triggered average of the neuron discharge (Fig. 11C & D) shows that the vestibular field potential is always present at constant latency, but the neuron fires only intermittently at the highest stimulus frequency. These interactions are potentially important in the elucidation of the mechanisms of information transfer within the vestibular nucleus during electrical stimulation. Individual secondary vestibular neurons are capable of following high stimulus frequencies during electrical stimulation, but do so with consistent latency only at higher stimulus current.

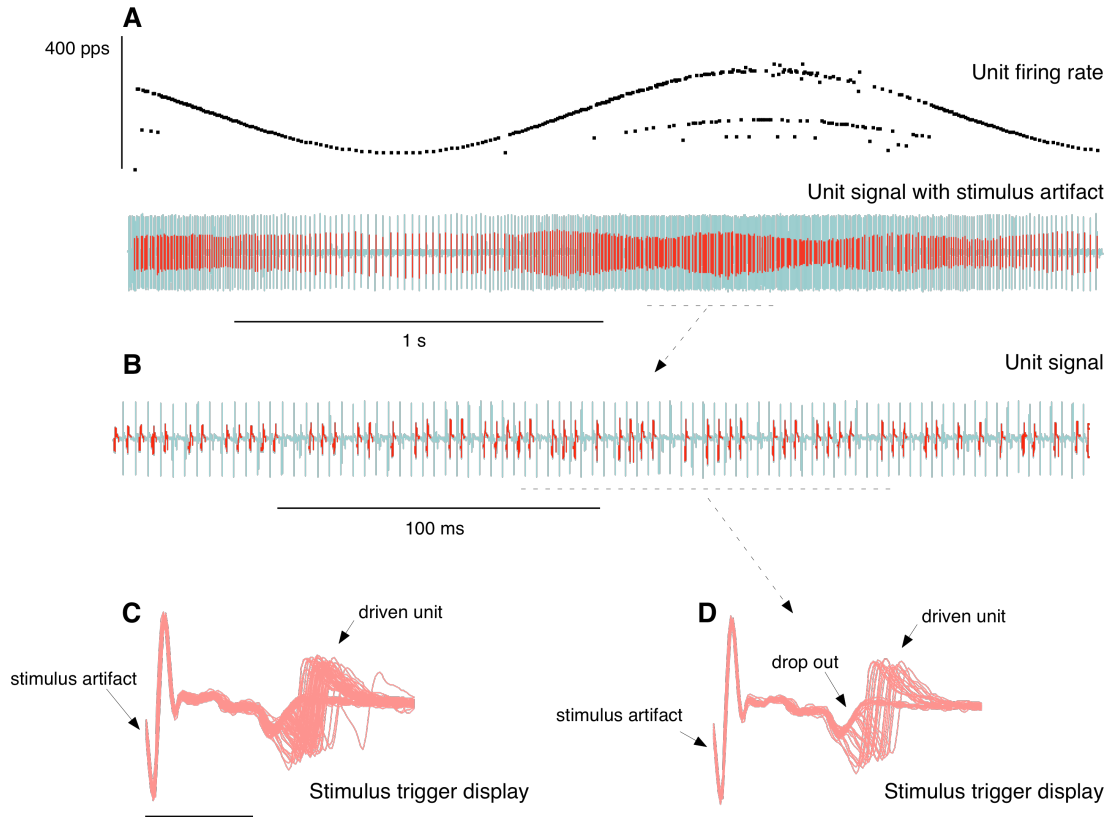


Figure 11. *Stimulation of the single vestibular neuron shown in Figs. 9 & 10 with a high frequency stimulation train at threshold current. The vestibular neuron (red) follows each low frequency stimulus pulse (grey) with a single spike discharge, but drops out occasionally at higher frequency. In A, the neuron discharge, stimulus artifact and neuron instantaneous firing frequency are displayed. In B, a portion of the stimulation at higher frequency (dotted line and arrow) is displayed at higher temporal resolution to show missed responses. In C, a stimulus triggered average of all of the spikes in B is displayed. In D, a stimulus triggered display of a subset of the spikes in B (dotted line and arrow) is displayed.*

On the other hand, when stimulus current is modulated at constant frequency, the neuron in Figs. 9–11 displays a simple alternation between two states (Fig. 12). For a 0.5 Hz train (50 pps) varying from 20 to 200 μA , the neuron follows the stimulus train reliably until reaching a stimulus current of 50 μA , and then drops out completely. This simple threshold-related behavior would produce a binary on and off signal. It is currently unclear how this signal is converted in the population average downstream to drive the sinusoidally modulated eye velocity we observed in our behavioral experiments.

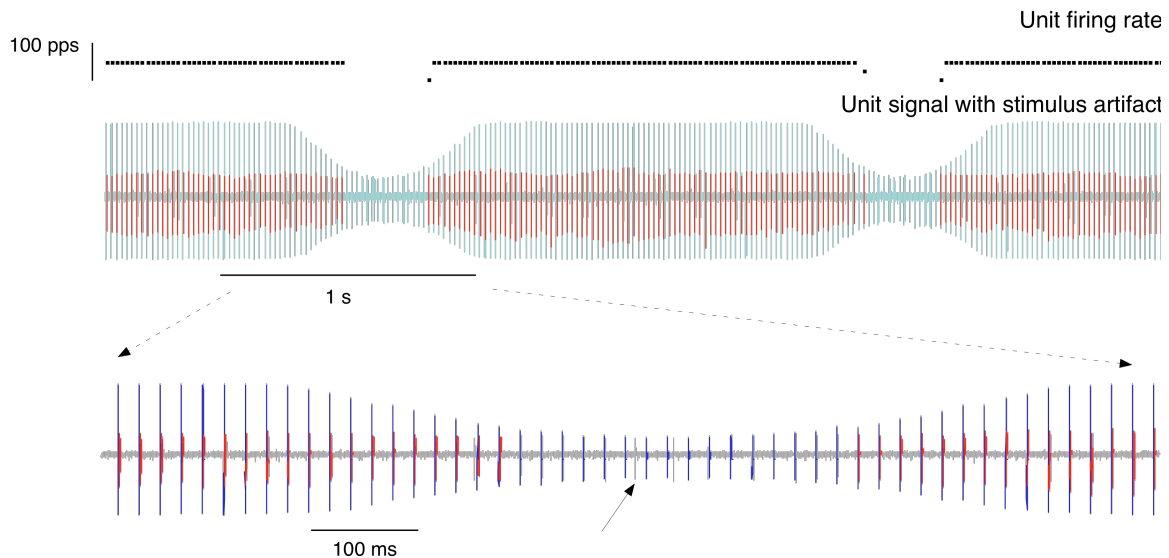


Figure 12: Stimulation of the vestibular neuron in figures 9-11 with amplitude modulated electrical stimulation of the lateral canal. The stimulation is modulated between 20 and 200 μA at a constant frequency of 50 pps. The stimulation parameters are 100 μs per phase, 8 μs gap. The top trace shows the instantaneous firing rate of the neuron, which is displayed in red in the middle recording trace against a background of grey stimulus artifact spikes. The artifact is modulated only at lower stimulus currents, and saturated at higher currents. The bottom trace displays a segment of the discharge displayed above (dotted arrows) at higher temporal resolution.

10. In this quarter, we received funding for submission of an IDE application to the Food and Drug Administration and a limited human trial of the vestibular prosthesis in 3 patients with Meniere’s disease. The grant, titled Clinical Feasibility of a Vestibular Prosthesis for Meniere's Disease, is a Translational Research Partnership Grant supported by the Wallace H Coulter Foundation. This study evaluates the feasibility of implantation of the current prosthesis for the treatment of Meniere’s disease in 3 patients who would otherwise undergo labyrinthectomy or nerve section to treat their disease. It is intended to collect preliminary data in support of an RO1 submission to the NIH.

11. In this quarter we wrote 2 papers. One paper was submitted for publication in Quarter 11, and the other will be submitted in Quarter 12. The titles of the papers and authors are listed below.

Nie, K., Rubinstein, J.T., Bierer, S.M., Ling, L., Oxford, T., Fuchs, A.F., Abbas, P.J., Phillips, J.O. Characterization of the electrically-evoked compound action potential of the vestibular nerve. To be submitted to *Otology & Neurotology*

Rubinstein, J.T., Bierer, S., Ling, L., Nie, K., Fuchs, A.F., Kaneko, C., Santos, F., Newlands, S., Risi, F., Oxford, T., Abbas, P., Phillips, J.O. Prosthetic Implantation of the Semicircular Canals with Preservation of Rotational Sensitivity: A "Hybrid" Vestibular Implant. To be submitted to *Otology & Neurotology*

Objectives for Quarter 12:

- 1. We will have submitted two additional papers and a neuroscience abstract.** We will have presented our data as a poster and invited presentation at the Conference on Implantable Prostheses 2009 in Lake Tahoe, California. We will have presented our data as an invited paper at the Combined Otological Spring Meetings in Phoenix, Arizona.
- 2. We will continue recording from secondary vestibular neurons in the vestibular nucleus during natural and electrical stimulation.** We will also record from higher order vestibular neurons in the ipsilateral and contralateral vestibular nucleus, and motoneurons in the abducens nucleus. Our objective will be to understand the extent to which higher order vestibular neurons are responsible for processing vestibular signals that result in eye movements.
- 3. We will implant two additional monkeys.** One animal will be implanted with fine wire electrodes, and one will be implanted with the new generation UW Cochlear vestibular implant. These animals will be used for canal plugging and aminoglycoside injection experiments, respectively.
- 4. We will evaluate head unrestrained responses to stimulation during natural movement behaviors in the two animals that are currently training with head and eye coils.** The head coils are mounted externally to the animals restraining lugs and the animals are trained to maintain stable head position and to track targets with combined eye and head movements.
- 5. We will examine nulling of optokinetically induced eye movement with electrical stimulation.** We will present full field visual motion with an optokinetic drum and cancel the resulting nystagmus during drum rotation in the light (OKN), and in the dark following prolonged drum stimulation (OKAN) to explore empirically the relationship between vestibular, optokinetic, and electrical stimulation inputs to the velocity storage mechanism in rhesus monkey.
- 6. We will begin our long term and real time stimulation experiments with the clinical processor and the PDA processor.** Initially, we will perform bench testing of the PDA processor to see if we can overcome the intermittent strobing of stimulation related to updating the processor. The new device should be capable of overcoming this

limitation. We will then test the PDA in vivo to confirm that this new strategy is effective. We will also drive the clinical processor in with analog signals from the head coil, to drive compensatory eye movements in real time.

7. Finally, we will get histology on three of our animals. We should be able to define more precisely the exact location of the neurons that we have recorded by reconstructing the location of electrolytic marking lesions placed adjacent to regions of interest.